

Generation of Complex, Static Solution Gradients in Microfluidic Channels

Hongkai Wu,^{*,‡} Bo Huang,[†] and Richard N. Zare[†]

Departments of Chemistry, Tsinghua University, Beijing, China 100084, and Stanford University, Stanford, California 94305-5080

Received December 16, 2005; E-mail: hkwu@mail.tsinghua.edu.cn

Molecular gradients of diffusible substances in solution play an important role in many processes, both chemical (e.g., crystal growth) and biological (e.g., chemotaxis,¹ morphogenesis² and nerve growth cone guidance³). However, precise molecular gradients that are steady in space and in time are difficult to create and maintain in free solutions. Diffusion of molecules in a solution continuously flattens any gradients (diffusion constants of molecules in aqueous solutions at room temperature are typically $\sim 10^{-6}$ – 10^{-7} cm²/s). Transient chemical gradients have been created in solutions by local delivery of reactants⁴ and steady-state pH gradients by electrolysis of water.⁵

Two approaches are commonly used to establish generic chemical gradients and maintain them in solution. A Dunn chamber and its variations form stable gradients by creating an initial stabilization period followed by slow decay.⁶ Simple profiles of the gradients created in this way are determined by the diffusion of molecules between separate reservoirs. Alternatively, Whitesides and co-workers⁷ use microfluidic channels to repetitively mix and split solutions of different concentrations, thereby generating a stable gradient perpendicular to the flow direction. The major innovation in this method is that, by manipulating the cycles of splitting and mixing, one can set up complex gradients. A crucial requirement is to maintain a constant flow in the channel.

We describe here a convenient technique that combines soft lithography with microfluidics to generate, accurately and in a known manner, a complex and steady gradient in a static solution. This approach eliminates unwanted effects associated with constant flow. Figure 1A illustrates the concept. Consider a surface with a constant concentration gradient \vec{G}_0 . For simplicity, let the vector \vec{G}_0 point along the x axis. The magnitude of the directional derivative at an angle θ measured from the x axis then ranges from $-G_0$ to $+G_0$ (Figure 1B). To set the concentration profile inside a channel to have a particular form, we design the path of the channel so that the concentration gradient along the direction of the channel at each point matches the desired concentration derivative. Specifically, a channel direction along the y axis does not affect the concentration, whereas that along the x axis causes the maximum change with distance.

The microfluidic device is fabricated in poly(dimethylsiloxane) (PDMS) by soft lithography⁸ with three parts (Figure 1C,D). The top is a PDMS piece with a chamber that opens to the bottom and connects to a reservoir at each end. The middle is a thin layer of hydrogel. After sealing the chamber with a flat PDMS substrate, we fill the chamber with a melted agarose solution (1% in water) that gels at room temperature. The bottom consists of another PDMS piece that is patterned with microfluidic channels (filled) on the surface. The top and bottom are sealed to each other conformally, with the hydrogel layer sandwiched between them, so that the channels are in close contact with the gel. After the device is assembled (Figure 1C), one reservoir is filled with a solution at

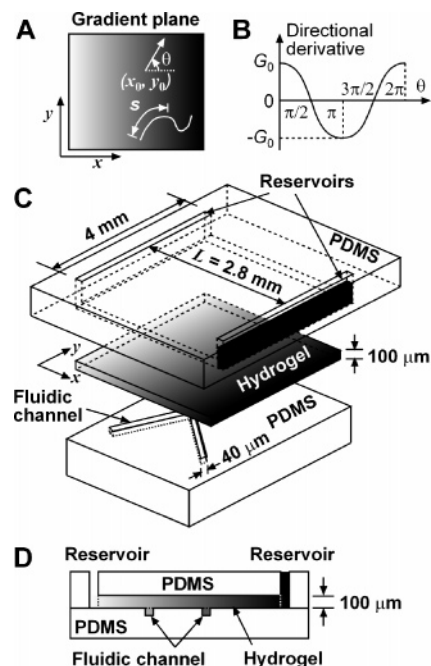


Figure 1. (A) Sketch of a 2D plane with a gradient built on its surface along the x axis. At a point (x_0, y_0) , the exact value of the directional derivative depends on its direction, which is defined by the angle θ . An arc length along a channel is denoted s . (B) Relation between directional derivative and angle θ when the surface gradient is linear along the x axis. The angle θ is measured counterclockwise from the x axis (shown in A). (C) Schematic diagram of a microfluidic device for generating complex static gradients in solution along microchannels. The three layers in the device are separated to show each layer clearly. Inlets can be formed on the bottom PDMS piece for the introduction of cells into the channels. (D) Cross section of an assembled device.

high concentration (C_1) and the other with a solution at low concentration (C_0). Molecules diffuse through the hydrogel and eventually reach equilibrium.

The layer of hydrogel serves three purposes. First, it offers a space for the diffusion of molecules. The molecules and the hydrogel should be compatible with each other; the molecules are water-soluble and smaller than the gel pores. Second, the gel prevents unwanted flow caused by hydraulic pressure from the liquid height difference in the reservoirs and local convective flows, which can disturb and even completely destroy established gradients. Third, the gel forms a physical barrier to a biological object (e.g., a blood cell) under study by containing the object in the channel.

We estimate the time to reach equilibrium from the relation

$$2Dt = L^2 \quad (1)$$

where D is the diffusion constant, t the time for equilibrium, and L the distance between the reservoirs. For $D \approx 10^{-6}$ cm²/s and $L = 2.8$ mm, t is ~ 10 h. Fresh solutions are reloaded into the reservoirs every 3 h to maintain concentrations in the reservoirs.

[‡] Tsinghua University.
[†] Stanford University.

The motion of molecules across the hydrogel between the two reservoirs in Figure 1C can be treated as one-dimensional (1D) diffusion along the x axis:

$$\partial C(x,t)/\partial t = D \partial^2 C(x,t)/\partial x^2 \quad (2)$$

where $C(x,t)$ is the local concentration at position x at time t . At equilibrium, $\partial C(x,t)/\partial t = 0$, and the local concentration can be written as $C(x)$ because it is independent of t . With the boundary conditions of $C(0) = C_0$ and $C(L) = C_1$, the solution to this differential equation gives a linear relation between the concentration and the position on the x axis:

$$C(x) = Kx + C_0 \quad (3)$$

where the constant $K = (C_1 - C_0)/L$ (eq 3) gives the concentration profile and shows that the equilibrium local concentration is independent of the diffusion coefficients of the species. Let us imagine that we put a thin channel in contact with the hydrogel. Molecules will diffuse into the channel and generate a concentration gradient which is the same as that in the gel.

This gradient in the channel induces additional concentration flux. Provided that the thickness of the channel is much smaller than that of the hydrogel, this flux will be much smaller than that in the hydrogel and will not perturb the established concentration profile (eq 3). Moreover, the thickness of the channel needs to be small compared to its length so that the concentration profile in the channel is the same at different depths. In practice, these conditions are readily satisfied.

The gradient in the solution is the concentration variation along the channel, i.e., the derivative of the concentration over the arc length (s) (Figure 1A) of the channel. If the microchannel has a profile that is described by $y = f(x)$, the solution gradient $G(s)$ at a location (x, y) in the channel is described by

$$s(x) = \int [1 + (dy/dx)^2]^{1/2} dx \quad (4)$$

$$G(s) = dC/ds = (dC/dx)/(ds/dx) = K/[1 + (dy/dx)^2]^{1/2} \quad (5)$$

$$C(s) = K \int [1 + (dy/dx)^2]^{-1/2} ds \quad (6)$$

Equation 6 shows our ability to control the concentration profile in a channel by designing its shape.

We use a fluorescent dye, Alexa Fluor (AF) 647 (Invitrogen), in a few typical channels (Figure 2A) to illustrate this method. The left reservoir is loaded with a buffer solution and the right with a concentrated solution of this dye. After the loaded device is left overnight in the dark at room temperature to reach equilibrium, we measure the fluorescence intensity along the microfluidic channels with a confocal fluorescence microscope (see Supporting Information). We use the concentration along the straight channel as a standard to calibrate the fluorescence intensity. The concentration profiles along more complex channels are given in Figure 2B. For comparison, Figure 2B also shows the calculated concentration curves of these channels, based on eq 6. The calculation (see Supporting Information) and the experimental data match closely.

We have also built different gradients of proteins in the same channel. Figure 2C shows the gradient profile of AF 647-labeled bovine serum albumin (BSA, Invitrogen) along a W-shaped channel. Complex gradients of multiple species in one channel can be produced by filling the reservoirs with different types of molecules (Figure 2D). More than two reservoirs could be used to form even more complicated gradients of different molecules. All these concentration gradients along the channel can be accurately designed and calculated.

Moreover, we expect that our methodology can be extended to the generation of other types of gradients. For example, we can

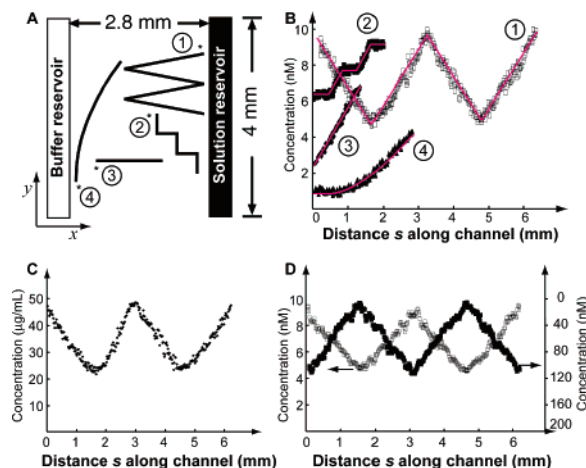


Figure 2. Static chemical gradients in solution along microfluidic channels. (A) Schematic illustration of the position of each channel relative to the reservoirs, which are 2.8 mm apart. The positions and lengths of all channels (1, W-shaped; 2, steplike; 3, straight; and 4, parabolic) and both reservoirs are to scale. All channels have a cross section of $40 \mu\text{m} \times 40 \mu\text{m}$. The asterisk indicates the starting end of each channel when measuring the concentration profile. (B) Concentration profiles of AF 647 against the distance along the channels. Red lines show the calculation curves of concentration in the channels. (C) Concentration profile of AF 647-labeled BSA against the distance along the W-shaped channel. The solution reservoirs in panels B and C contain 10 nM AF 647 and 50 $\mu\text{g/mL}$ BSA, respectively. (D) Concentration profiles of AF 647 (\square) and AF 555 (\blacksquare) against the distance along the W-shaped channel. All solutions are in Hepes (pH ~ 7.5) buffer. The right reservoir is filled with 10 nM AF 647 and the left with 200 nM AF 555.

use the underside of the channel to introduce a gradient of a second species. It is also possible to introduce thermal gradients because they satisfy the same diffusion equations.

This work demonstrates a convenient method for building various complex gradients of diffusible molecules in static solutions along microfluidic channels. This method has the following advantages over alternative techniques: (1) it can generate arbitrary gradient profiles along a channel in the range of the gradient between the reservoirs; (2) the gradient can be accurately calculated and designed with simple equations; (3) the solution that bears the gradient is static (a static solution not only prevents any effect from fluid flow in a study but is also crucial for a study in solution on nonattached subjects, such as nonadherent cells); and (4) the gradient is spatially and temporally stable over essentially indefinite periods of time.

Acknowledgment. This work is supported by the National Science Foundation under NSF BES-0508531.

Supporting Information Available: Experimental details including the experimental setup of confocal fluorescence microscopy, and calculated concentration profiles shown in Figure 2B. This material is available free of charge via the Internet at <http://pubs.acs.org>.

References

- Boyd, S. J. *Exp. Med.* **1962**, *115*, 453–466.
- Neumann, C.; Cohen, S. *Bioessays* **1997**, *19*, 721–729.
- Baier, H.; Bonhoeffer, F. *Science* **1992**, *255*, 472–475.
- Olofsson, J.; Bridle, H.; Sinclair, J.; Granfeldt, D.; Sahlin, E.; Orwar, O. *Proc. Natl. Acad. Sci. U.S.A.* **2005**, *102*, 8097–8102.
- Cabrera, C. R.; Finlayson, B.; Yager, P. *Anal. Chem.* **2001**, *73*, 658–666.
- Zicha, D.; Dunn, G. A.; Brown, A. F. *J. Cell Sci.* **1991**, *99*, 769–775.
- Zigmond, S. H. *J. Cell Biol.* **1977**, *75*, 606–616.
- Jeon, N. L.; Baskaran, H.; Dertinger, S. K. W.; Whitesides, G. M.; van de Water, L.; Toner, M. *Nat. Biotechnol.* **2002**, *20*, 826–830.
- Jiang, X.; Xu, Q.; Dertinger, S. K. W.; Stroock, A. D.; Fu, T.; Whitesides, G. M. *Anal. Chem.* **2005**, *77*, 2338–2347.
- Xia, Y.; Whitesides, G. M. *Angew. Chem., Int. Ed.* **1998**, *37*, 550–575.
- Wu, H.; Odom, T. W.; Chiu, D. T.; Whitesides, G. M. *J. Am. Chem. Soc.* **2003**, *125*, 554–559.

JA0585300